SUPPLEMENTARY METHODS

Antibodies

Monoclonal antibodies used were against transglutaminase 2 (TG2) (IA12, University of Sheffield, UK; CUB 7402, MA5-12739 Invitrogen, UK), α-smooth muscle actin (α-SMA) [1A4] (ab7817, Abcam, UK) and flotillin-2 (FLOT2) (610383, BD Transduction Laboratories, UK). Polyclonal antibodies used were against syndecan-4 (SDC4) (ab24511, Abcam, UK), TG2 (ab421, Abcam, UK), cyclophilin-A (ab41684, Abcam, UK), β-Tubulin (ab6046, Abcam, UK), hemagglutinin (HA) (C29F4, Cell Signaling Technology, UK) and GFP (ab290, Abcam, UK).

Unilateral ureteric obstruction

Experimental unilateral ureteric obstruction (UUO) was performed in TG2-KO and control (Wild Type, WT) C57BL/6J mice as described by Vielhauer *et al*. (2001).[1] To perform UUO, mice were anaesthetized with 5% isoflurane and anesthesia maintained with 2% isoflurane during the surgical process. The left ureter of the mice was obstructed using a legating clip (Hemoclip Plus, Weck Closure Systems). ADEPT® [4% (w/v) icodextrin solution] was dispensed in the peritoneum to prevent post-surgical adhesions prior to closing. The muscle wall was sealed with continuous stitching and skin wound closed with interrupted stitching using absorbable sutures. After the procedure, buprenorphine (0.1 mg/kg) was administered to the mice for pain-relieving. Animal were allowed free access to standard rodent chow and tap water. Mice were sacrificed and the left kidneys harvested 21 days post-operation. All experimental procedures were carried out under license in accordance with regulations laid down by Her Majesty's Government, UK (Animals Scientific Procedures Act ASPA, 1986), and were

approved by the University of Sheffield Animal Ethical Review Committee (ASPA Ethical Review Process) and Nottingham Trent University Ethical Review Committee (ASPA Ethical Review Process).

Fibrosis measurement

Kidneys were fixed in 10% formalin for 15 h at room temperature and washed with phosphate buffer saline (PBS) pH 7.4 prior to paraffin embedding. Kidney was then sectioned and stained with Masson's trichrome, which marks collagenous material blue and nuclei, fibers, erythrocytes and elastin red/pink. Images of Masson's trichrome stained kidney section were randomly acquired using Olympus BX61 microscope. Quantification of kidney fibrosis was undertaken using multiphase image analysis as previously described using Cell F software [2](Olympus, Germany).

Detection of TGF-β activity in kidney homogenates by mink lung epithelial cell (MLEC) bioassay

A 10% (w/v) kidney homogenate was prepared in homogenization buffer [0.25 M sucrose, 10 mM Tris-HCl, 1 mM $MgCl_2$, 2 mM EDTA, pH 7.4] containing 1:100 (v/v) protease inhibitors cocktail (P8340, Sigma, UK). Mechanical homogenization was performed on ice using an Ultra Turrax T25 homogenizer (Merck, UK). Each homogenate was centrifuged at 1000 g for 5 min at 4°C to remove large particulates, then the supernatant diluted 1:10 in sterile-filtered (2 µm, Sartorius Stedim, UK) serum-free DMEM with 0.1% (w/v) BSA. 100 µL of this solution was assayed for the presence of active soluble TGF-β by application on the mink lung epithelial cell line (MLEC) of the TGF-β quantification system[3] in a 96-well plate ($5x10^4$ cells/well) for 22 h. Cells were then washed twice with PBS and lysed in 1X

Reporter Lysis Buffer (Promega, UK). 50 µL of cell lysate were mixed to an equal volume of luciferase substrate (Promega, UK) and light emission measured with Polarstar Optima luminometer (BMG Labtech, UK). Total TGF-β was measured following acid treatment of the kidney homogenate and incubation with the MLEC system.[4,5]

SWATH acquisition mass spectrometry and data analysis of TG2-immunopreciptates

Tryptic peptides from TG2 immunoprecipitates were subjected to reverse-phase high-pressure liquid chromatography electrospray ionization tandem mass spectrometry (RP-HPLC-ESI-MS/MS) using a TripleTOF 5600+ mass spectrometer from SCIEX (Canada). The mass spectrometer was used in two different modalities depending on the stage of the experiment: data dependent acquisition (DDA) mode was employed at the beginning for spectral library construction, while SWATH® 2.0 - data independent acquisition (DIA) mode for used for the quantitation.[6]

RP-HPLC mobile phases were solvent A [2% (v/v) LC/MS grade acetonitrile, 5% (v/v) DMSO and 0.1% (v/v) formic acid in LC/MS grade water] and solvent B [LC/MS grade acetonitrile containing 5% (v/v) DMSO and 0.1% (v/v) formic acid]. Samples were injected with an Eksigent nanoLC 425 system using NanocHiPLC columns (Eksigent, USA) with trap and elute system (200 µm × 0.5 mm trap column and 75 µm × 15 cm analytical column packed with 3 µm ChromSP C-18 media - 300 Å). Samples were loaded onto the trap column at 5 µL/min for 3 min in 100% solvent A, then were eluted from the analytical column at a flow rate of 300 nL/min using an increasing linear gradient of solvent B over solvent A, going from 5% to 35% in a total time of 60 min (SWATH-DIA) or 120 min (Spectral

library production by DDA). Regeneration and re-equilibration of the column were performed by loading 90% solvent B for 10 min followed by 5% solvent B for 10 min. Autocalibration was performed by the MS every four samples using an injection of a standard of 25 pmol β-galactosidase digest. The electrospray ionization was carried out using PicoTIP nanospray emitters uncoated SilicaTips (New Objective, USA) with voltage set to +2400 V.

A spectral library was produced by DDA on a pool of all samples, in high sensitivity mode. DDA mass spectrometry files were searched using ProteinPilot 4 (SCIEX) and the analysis was conducted by the software with an exhaustive identification strategy, searching the UniProt/Swiss-Prot database (January 2014 release) for murine species. The generated file was imported into PeakView 2.0 software (SCIEX) as an ion library and spiked in iRT retention time standards (Biognosys, Switzerland), after filtering for false discovery rate (FDR) of 1% and excluding shared peptides.

Five TG2-IP samples per treatment were subjected to cyclic DIA using static SWATH windows of *m/z* = 15. Thirty-four static SWATH windows from 400 to 900 *m/z* were used with an accumulation time of 96 ms, giving a cycle time of 3.3 s. During different cycles, the initial survey scan (TOF-MS) was performed for each window, and subsequently the MS/MS experiments was carried out on the totality of the precursors detected in the SWATH window using rolling collision energy.[6]

Spectral alignment and targeted data extraction was performed in PeakView 2.0 using the reference spectral library generated by DDA in a pool of TG2-IP samples. SWATH data was processed using an extraction window of 12 min and applying these parameters: 100 peptides, 5 transitions, peptide confidence > 99%, exclusion of shared peptides, and XIC width set at 50 ppm. The output consisted of three different quantification files representing the intensity of the individual

transitions (the area under the intensity curve), of the different peptides (cumulative peak area of the transitions) and of the proteins (cumulative peak area of the peptides). To identify the proteins significantly associated to TG2, a z-test statistical analysis was performed on the normalized protein peak areas (as outlined in the next section), using the TG2-KO data as background.

Z-test statistical analysis

The significance of protein association with TG2 was determined by z-test analysis[7] of the five independent SWATH data acquisition mass spectrometry experiments performed on TG2-IP, using the TG2-null mice as background control. First, the protein peak area of every detected protein was normalized within the whole experiment using a Z-transformation: each intensity value was transformed using the natural log transformation and then normalized by subtracting the average of the entire population (μ) and dividing for the standard deviation of the entire population (σ), as shown in the equation (1) below. ΔZ values were then calculated by subtracting TG2-KO Z-score from WT Z-score for each protein in the same treatment (sham or UUO) (equation 2). Finally, the z-test (equation 3a) was performed on the five experiments together, to compare WT and TG2-KO data in the same treatment: the average of the ΔZ for the protein in the different experiments was divided by the standard error of the ΔZ in the different experiments (equation 3b). Results were then plotted on a normal distribution curve to obtain probability values (p-values). Proteins with p-value lower than 0.05 detected in at least 4 out of 5 experiments ($n \geqslant 4$) were regarded as significantly associated with TG2, meaning that the protein can be considered a specific partner (directly or indirectly associated) for the enzyme.

$$(1)\ Z\ score = \ Z_i = \frac{X_i - \mu}{\sigma}$$

$$(2)\ \Delta Z_i = Z_{WT,\,i} - Z_{KO,\,i}$$

$$(3a)\ Z\_test_i = \frac{X_i - H_0}{SE}$$

Since $H_0: \Delta Z = 0 \rightarrow \ Z_{WT} - Z_{KO} = 0$ *(no differences between WT and TG2-KO)*

$$(3b)\ Z\_test_i = \frac{\Delta Z_i}{SD_i \Big/ \sqrt{N}}$$

SWATH acquisition mass spectrometry and data analysis of kidney proteomes

Kidney lysates were analyzed by RP-HPLC-ESI-MS/MS using a TripleTOF 5600+ mass spectrometer as outlined before, with some modification in the protocol. Samples were directly injected onto an YMC Triart-C18 column (25 cm, 2 µm, 300 µm i.d) at 5 µL/min using microflow LC system (Eksigent ekspert nano LC 425) and an increasing linear gradient of solvent B over solvent A going from 2% to 40% in a total time of 60 min (SWATH-DIA) or 120 min (spectral library production by DDA). A spectral library was produced by DDA on a pool of all samples in high sensitivity mode and DDA mass spectrometry files were searched using ProteinPilot 5 (SCIEX). The analysis was conducted by the software with an exhaustive identification strategy, searching the UniProt/Swiss-Prot database (March 2016 release) for murine species. The generated file was imported into PeakView 2.0 software (SCIEX) and spiked in iRT as outlined before.

SWATH-DIA was executed on four kidney lysates per treatment (WT or TG2-KO, UUO or sham operated). DIA was performed using 40 variable SWATH windows. Spectral alignment and targeted data extraction from the SWATH data was performed in OneOmics (SCIEX) using the reference spectral library produced

by DDA. SWATH data were processed using an extraction window of 5 min and applying the following parameters: 6 peptides/protein, 6 transitions, peptide confidence of >99%, exclude shared peptides, and XIC width set at 75 ppm. Analysis of the differentially expressed proteins between the different treatments were carried out using SCIEX OneOmics cloud processing software, as the ratio of protein peak area in UUO kidney lysates over the protein peak area of the same protein in sham operated condition [$\log_2$(UUO/Sham)]. Data were regarded as differentially expressed at 0.8 (80%) confidence level.

Bioinformatic Analysis

Proteins were clustered in categories depending on their known main biological function. This was performed by manual search of the protein IDs into the UniProt Knowledgebase (UniProtKB) (www.uniprot.org[8]; UniProt Consortium, 2015) and GeneCards® database (www.genecards.org[9]). Functional classification and pathway analysis was performed using two different open source bioinformatics resources: DAVID (Database for Annotation, Visualization, and Integrated Discovery) bioinformatics resource 6.7 (http://david.abcc.ncifcrf.gov)[10] and PANTHER (Protein ANalysis THrough Evolutionary Relationships) database (www.pantherdb.org).[11] In both cases, the whole *Mus musculus* genome was employed as background list. Functional enrichment analysis was performed in PANTHER using PANTHER protein class terms. Pathway overrepresentation analysis was performed using DAVID bioinformatics resource by comparing the representation of the different Kyoto Encyclopedia of Genes and Genomes (KEGG, www.genome.jp/kegg) terms (KEGG_PATHWAY) to the expected pathway representation in *Mus musculus*.

In order to identify clusters and networks of interacting proteins, known and predicted protein-protein interactions were investigated using STRING (Search Tool for the Retrieval of INteracting Genes/proteins) database v10 (http://string-db.org).[12] The network was produced by using confidence level higher than the default 0.4 and by removing all the unconnected proteins and the small unconnected networks. The network was exported and analyzed using the open source software Cytoscape v. 3.0.2 (www.cytoscape.org), to visualize the protein clusters and assign specific colors to the nodes corresponding to the different functional clusters.

Isolation and characterization of extracellular vesicles from cell medium

To extract extracellular vesicles (EVs) from cell medium, cells were cultured until 80% confluent. At this stage, cell monolayers were washed twice with PBS to remove every fetal bovine serum (FBS) trace, the medium was replaced with serum-free DMEM containing L-glutamine and penicillin/streptomycin, and cells were cultured for additional 36 h.

After incubation, medium was collected and supplemented with protease inhibitors (Roche, UK). Cells were washed with PBS, scraped in PBS, and the pellet collected by centrifugation at 500 g for 5 min. Medium was centrifuged three times at 300 g for 10 min at 4°C to remove remaining cells, and supernatant (S1) was centrifuged at 1,200 g for 20 min at 4°C to remove large cell debris and apoptotic bodies (P2). Supernatant (S2) was centrifuged 10,000 g for 30 min at 4°C in order to collect the microvesicular (ectosomal) portion (P3), which supernatant (S3) was centrifuged at 110,000 g for 1 h at 4°C in order to collect the exosomes (P4)[13,14]. All pellets were collected and resuspended in 40 µL of the suitable buffer. After the last centrifugation, cleared medium (S4) was collected and proteins were

precipitated using trichloroacetic acid (TCA), as follows: 0.1 volume of TCA was added to the medium and incubated for 1 h on ice. The mixture was centrifuged for 5 min at 13,000 rpm, then pellet was washed with cold 100% acetone and centrifuged again for 5 min 13,000 rpm. Pellet (EV-free medium proteins and complexes) was air-dried and resuspended in 40 µL of the suitable buffer.

For EV analysis by tunable resistive pulse sensing (TRPS) (qNano, Izon), Nanopore NP150 (Izon) and calibration particles (1:1, 200 nm, Izon) were used to analyze exosomes while Nanopore NP300 (Izon) and calibration particles (1:1, 200nm) were used for ectosome analysis. Samples were measured at three pressure levels. The sizes and concentrations of particles were determined using the software provided by Izon (version 3.2).

Isolation of primary cells from WT and SDC4-null mice

Kidney glomeruli and tubules were isolated from wild type and SDC4$^{-/-}$ mice C57BL/6J mice using the method described by Fisher et al. [15] The kidney was perfused in situ with Dynabeads® which become wedged in the glomeruli. The cortex was isolated, disrupted and passed through sieves with the filtrate consisting of cortical tubular fragments and some glomeruli. Any glomeruli were removed and set aside by use of a strontium magnet. The remaining tubular fragments were plated in tissue culture dishes containing medium with low serum and growth supplements to stimulate epithelial cell proliferation. The primary tubular epithelial cells (TECs) grew out from tubules in the following medium: DMEM/F12, containing 0.5% heat-inactivated FBS (v/v), 100 U/mL penicillin, 100 µg/mL streptomycin, 22 mM L-glutamine, and supplemented with 10 µg/mL insulin, 5.5 µg/mL transferrin, 5 ng/mL sodium selenite (ITS supplement, Sigma, UK), 10 ng/mL epidermal growth factor (R&D Systems, UK), 5 pg/mL tri-

iodothyramine, 5 µg/mL dexamethasone, 12.5 µg/mL each of adenosine, cytosine, guanosine, uridine and 2.5 µg/mL amphotericin B. Primary fibroblasts grew out from tubules in Dulbecco's modified Eagle's medium:nutrient mixture F12 (DMEM/F12), containing 10% (v/v) heat-inactivated FBS (Biosera, UK), 100 IU/mL penicillin, 100 µg/mL streptomycin and 0.25 µg/mL amphotericin-B; Primary mesangial cells grew out from glomeruli in Roswell Park Memorial Institute (RPMI) 1640 medium containing 20% (v/v) heat-inactivated FBS, 2.2 mM L-glutamine, 1 mM sodium pyruvate, 0.075% (w/v) sodium bicarbonate, 15 mM HEPES, 100 IU/mL penicillin, 100 µg/mL streptomycin and 0.25 µg/mL amphotericin-B. All media were from Invitrogen, and the supplements from Sigma, unless otherwise stated.

Western blotting

10% (w/v) kidney homogenates were prepared in homogenization buffer [0.25 M sucrose, 10 mM Tris-HCl, 1 mM $MgCl_2$, 2 mM EDTA, pH 7.4] containing 1:100 (v/v) protease inhibitors cocktail (Sigma, UK). Mechanical homogenization was performed on ice, using an Ultra Turrax T25 homogenizer (Merck, UK). Cell lysates and EV lysates were prepared in in radiommunoprecipitation assay (RIPA) buffer [50 mM TRIS HCl pH 8, 150 mM NaCl, 1% (v/v) NP40 detergent solution, 0.5% (w/v) sodium deoxycholate, 0.1% (w/v) SDS] containing EDTA-free protease inhibitors (Roche, UK). Unless differently stated, equal amounts of proteins were resolved by SDS-PAGE [8% to 12% (w/v) acrylamide] under reducing and denaturing conditions. Immunodetection of the proteins of interest was performed by Western blot. After initial optimizations, typically the blot was cut horizontally and probed with different antibodies to minimize stripping and re-probing. Immunoreactive bands were detected by enhanced chemiluminescence (EZ-

chemiluminescence detection kit for HRP, Geneflow) after incubation with appropriate HRP-conjugated secondary antibody. Secondary antibodies were obtained from Dako (Denmark). Image acquisition was performed with a LAS4000 imaging system (GE Healthcare, UK).

Extracellular vesicle isolation form urine samples

Clinical cell-free urine samples from CKD patients characterized by stage 3 and 4 CKD (GFR loss higher than 4 mL/min per year; n=10) and controls (n=5) were obtained by informed consent for a study approved by the Research Ethics Committee of Sheffield University. EVs were isolated from 12 mL pools of cell-free urine following a protocol similar to that employed to isolate EVs from cell culture medium, with adaptations described by Sequeiros et al., 2017.[16] P3 (ectosomes) and P4 (exosome) pellets and the TCA-precipitated EV-free urine fraction (S4) were homogenized in RIPA buffer, proteins quantified (BCA assay) and equal amounts analyzed in reducing and denaturing conditions by Western blotting. All precautions to lower interference from DTT and urea were taken in the protein assay.

SUPPLEMENTARY FIGURES

Supplementary Figure 1. Specific TG2 partner proteins belonging to the nuclear membrane compartment (A) or with mitochondrial/peroxisomal membrane location (B). TG2 associated proteins in UUO or sham operated kidney membranes were defined by z-analysis ($p \leq 0.05$, $n \geq 4$) of n=5 independent experiments which combined TG2-IP and SWATH-MS, using the TG2-null mice as background control, as described in legend to Table 1. Membrane proteins previously reported to be exclusively located in nucleus (A) and in the mitochondrial or peroxisomal compartments (B) were manually selected from the SWATH-MS dataset according to the subcellular localization database "COMPARTMENTS" and UniProtKB. The presented histograms list proteins in order of significance of their association to TG2 (Log_{10} p-value) in UUO (red color histogram bars) and sham controls (grey color histogram bars).

Supplementary Figure 2. TG2 associated proteins in UUO-Enriched KEGG pathways likely to be involved in kidney fibrosis. Example of KEGG pathways (www.genome.jp/kegg/) overrepresented in the UUO kidney compared to sham operated kidney (with reference to Suppl. Table 4B). ECM-receptor interaction (A), regulation of the actin cytoskeleton (B). Red stars denote proteins significantly increased in the UUO kidney compared to the sham operated conditions (confidence > 80%). Blue stars denote proteins found to be significantly associated with TG2 ($p \leq 0.05$) in the UUO kidney membrane fraction.

Supplementary Figure 3. TG2 in extracellular vesicle fractions of NRK49F fibroblasts. NRK49F cells were grown in serum-free medium for 36 h without and

with supplementation of 10 ng/mL TGF-β1. After incubation, culture medium was collected and vesicular fraction separated by serial centrifugation as described in the Methods. All fractions were immunoprobed for TG2 and flotillin-2 (FLOT2).

Supplementary Figure 4. TG2 in extracellular vesicle fractions from urine. Ectosomal (P3) and exosomal (P4) fractions were isolated by serial centrifugation from pools of cell-free urine from healthy and CKD patients (stages 3-4), as described in the Suppl. methods. Proteins from EV-free urine (S4) were concentrated by TCA precipitation. Equal amounts of EV fractions and EV-free urine were immunoprobed with primary antibodies towards TG2 (mouse monoclonal CUB 7402) and FLOT2.

SUPPLEMENTARY TABLES

Supplementary Table 1. Ribosomal proteins (A and B) and immunoglobulins (C) associated with TG2 in the UUO and sham kidney membranes. The association was evaluated as described in legend to Table 1. Proteins are denoted by full gene name and ID, and listed according to specificity of the interaction with TG2. U, TG2-associated proteins uniquely found in UUO membranes; S, TG2-associated proteins uniquely found in Sham operated membranes; U/S, TG2-asociated proteins in UUO and sham control membranes.

Supplementary Table 2. UUO versus sham kidney proteome – proteins increasing upon UUO (UUO/sham > 1). The UUO and sham operated kidney proteome was resolved by SWATH acquisition MS as described in the Methods. Proteins significantly increased in UUO kidneys at confidence ≥ 80% are listed

according to UUO/Sham ratio as calculated by SCIEX OneOmics cloud processing software. The absolute protein peak area variation ($2^{Abs\ [log_2(UUO/Sham)]}$) is here shown. Red cells represent a higher signal in UUO compared to sham, and proteins are sorted by descending values. Yellow represent the confidence; a confidence ≥ 80% was regarded as significant.

Supplementary Table 3. UUO versus sham kidney proteome – proteins decreasing upon UUO (UUO/sham < 1). The UUO and sham kidney proteome was resolved and UUO/Sham ratio expressed as described in legend to Suppl. Table 2. The absolute peak area variation ($2^{Abs\ [log_2(UUO/Sham)]}$) is here shown. Green cells represent a lower signal in UUO compared to sham operated kidneys and proteins are sorted by descending values.

Supplementary Table 4. Functional classes and pathways significantly overrepresented in the UUO proteome. (A) PANTHER protein class overrepresentation analysis (p≤0.05) on the pool of UUO upregulated (N=195) and downregulated (N=458) proteins (respectively shown in Suppl. Table 2 and Suppl. Table 3). (B) KEGG pathways overrepresentation analysis (p≤0.05), performed with DAVID functional annotation, on the pool of UUO-upregulated proteins.

SUPPLEMENTARY MOVIES

Supplementary Movie 1. Dependence of TG2 vesicular trafficking on Syndecan-4 in primary TECs. Wild type (WT) and SDC4-KO ($SDC4^{-/-}$) primary TECs were transiently transfected with 5 µg of pEGFP-N1-TG2 plasmid by

354 employing TransIT® transfection reagent (Mirus Bio). In order add back SDC4 in
355 SDC4$^{-/-}$ TECs, cells were co-transfected with 5 µL pcDNA3.1(+)-hSdc4 plasmid.
356 Time-lapse video clips were taken for WT TEC (A), SDC4$^{-/-}$ (B) and SDC4
357 transfected SDC4$^{-/-}$(C) TEC expressing EGFP-TG2 (green). EGFP-TG2 was
358 recruited in globular elements protruding and retracting from the PM (A). Arrows
359 indicate the formation of EGFP-TG2 vesicular blebbing on the edge of the cells.
360 EGFP-TG2 was less dynamic and appeared to be retained in the cytosol in the
361 SDC4-null TECs, which also had less budding activity than the wild type TECs (B).
362 Add back of SDC4 in SDC4-null TECs restored EGFP-TG2 vesicular blebbing and
363 "budding" reconstituted to wild type levels (C).
364
365
366 **SUPPLEMENTARY DATA**
367
368 **Supplementary Data 1. Original processed data and z-test analysis for the**
369 **TG2 interactome in UUO and sham operated kidney membranes.**
370
371 **Supplementary Data 2. Original processed for the kidney proteome in**
372 **UUO and sham operated conditions.**

373 Reference List

374

375 1. Vielhauer, V, Anders, HJ, Mack, M, Cihak, J, Strutz, F, Stangassinger, M, Luckow, B, Grone, HJ,
376 Schlondorff, D: Obstructive nephropathy in the mouse: progressive fibrosis correlates with
377 tubulointerstitial chemokine expression and accumulation of CC chemokine receptor 2- and
378 5-positive leukocytes. *J Am Soc Nephrol,* 12**:** 1173-1187, 2001.
379 2. Huang, L, Haylor, JL, Hau, Z, Jones, RA, Vickers, ME, Wagner, B, Griffin, M, Saint, RE, Coutts, IG, El
380 Nahas, AM, Johnson, TS: Transglutaminase inhibition ameliorates experimental diabetic
381 nephropathy. *Kidney Int,* 76**:** 383-394, 2009.
382 3. Abe, M, Harpel, JG, Metz, CN, Nunes, I, Loskutoff, DJ, Rifkin, DB: An assay for transforming growth
383 factor-beta using cells transfected with a plasminogen activator inhibitor-1 promoter-
384 luciferase construct. *Anal Biochem,* 216**:** 276-284, 1994.
385 4. van Waarde, MA, van Assen, AJ, Kampinga, HH, Konings, AW, Vujaskovic, Z: Quantification of
386 transforming growth factor-beta in biological material using cells transfected with a
387 plasminogen activator inhibitor-1 promoter-luciferase construct. *Anal Biochem,* 247**:** 45-51,
388 1997.
389 5. Scarpellini, A, Huang, L, Burhan, I, Schroeder, N, Funck, M, Johnson, TS, Verderio, EA: Syndecan-4
390 knockout leads to reduced extracellular transglutaminase-2 and protects against
391 tubulointerstitial fibrosis. *J Am Soc Nephrol,* 25**:** 1013-1027, 2014.
392 6. Gillet, LC, Navarro, P, Tate, S, Rost, H, Selevsek, N, Reiter, L, Bonner, R, Aebersold, R: Targeted data
393 extraction of the MS/MS spectra generated by data-independent acquisition: a new concept
394 for consistent and accurate proteome analysis. *Molecular & cellular proteomics : MCP,* 11**:**
395 O111 016717, 2012.
396 7. Cheadle, C, Vawter, MP, Freed, WJ, Becker, KG: Analysis of microarray data using Z score
397 transformation. *The Journal of molecular diagnostics : JMD,* 5**:** 73-81, 2003.
398 8. Magrane, M, UniProt, C: UniProt Knowledgebase: a hub of integrated protein data. *Database : the*
399 *journal of biological databases and curation,* 2011**:** bar009, 2011.
400 9. Safran, M, Dalah, I, Alexander, J, Rosen, N, Iny Stein, T, Shmoish, M, Nativ, N, Bahir, I, Doniger, T,
401 Krug, H, Sirota-Madi, A, Olender, T, Golan, Y, Stelzer, G, Harel, A, Lancet, D: GeneCards Version
402 3: the human gene integrator. *Database : the journal of biological databases and curation,*
403 2010**:** baq020, 2010.
404 10. Dennis, G, Jr., Sherman, BT, Hosack, DA, Yang, J, Gao, W, Lane, HC, Lempicki, RA: DAVID: Database
405 for Annotation, Visualization, and Integrated Discovery. *Genome biology,* 4**:** P3, 2003.
406 11. Mi, H, Muruganujan, A, Casagrande, JT, Thomas, PD: Large-scale gene function analysis with the
407 PANTHER classification system. *Nat Protoc,* 8**:** 1551-1566, 2013.
408 12. Szklarczyk, D, Franceschini, A, Wyder, S, Forslund, K, Heller, D, Huerta-Cepas, J, Simonovic, M, Roth,
409 A, Santos, A, Tsafou, KP, Kuhn, M, Bork, P, Jensen, LJ, von Mering, C: STRING v10: protein-
410 protein interaction networks, integrated over the tree of life. *Nucleic acids research,* 43**:** D447-
411 452, 2015.
412 13. Bianco, F, Perrotta, C, Novellino, L, Francolini, M, Riganti, L, Menna, E, Saglietti, L, Schuchman, EH,
413 Furlan, R, Clementi, E, Matteoli, M, Verderio, C: Acid sphingomyelinase activity triggers
414 microparticle release from glial cells. *The EMBO journal,* 28**:** 1043-1054, 2009.
415 14. Benussi, L, Ciani, M, Tonoli, E, Morbin, M, Palamara, L, Albani, D, Fusco, F, Forloni, G, Glionna, M,
416 Baco, M, Paterlini, A, Fostinelli, S, Santini, B, Galbiati, E, Gagni, P, Cretich, M, Binetti, G,
417 Tagliavini, F, Prosperi, D, Chiari, M, Ghidoni, R: Loss of exosomes in progranulin-associated
418 frontotemporal dementia. *Neurobiology of aging,* 40**:** 41-49, 2016.
419 15. Fisher, M, Jones, RA, Huang, L, Haylor, JL, El Nahas, M, Griffin, M, Johnson, TS: Modulation of tissue
420 transglutaminase in tubular epithelial cells alters extracellular matrix levels: a potential
421 mechanism of tissue scarring. *Matrix biology : journal of the International Society for Matrix*
422 *Biology,* 28**:** 20-31, 2009.

16. Sequeiros, T, Rigau, M, Chiva, C, Montes, M, Garcia-Grau, I, Garcia, M, Diaz, S, Celma, A, Bijnsdorp, I, Campos, A, Di Mauro, P, Borros, S, Reventos, J, Doll, A, Paciucci, R, Pegtel, M, de Torres, I, Sabido, E, Morote, J, Olivan, M: Targeted proteomics in urinary extracellular vesicles identifies biomarkers for diagnosis and prognosis of prostate cancer. *Oncotarget,* 8**:** 4960-4976, 2017.

Supplementary Figure 1

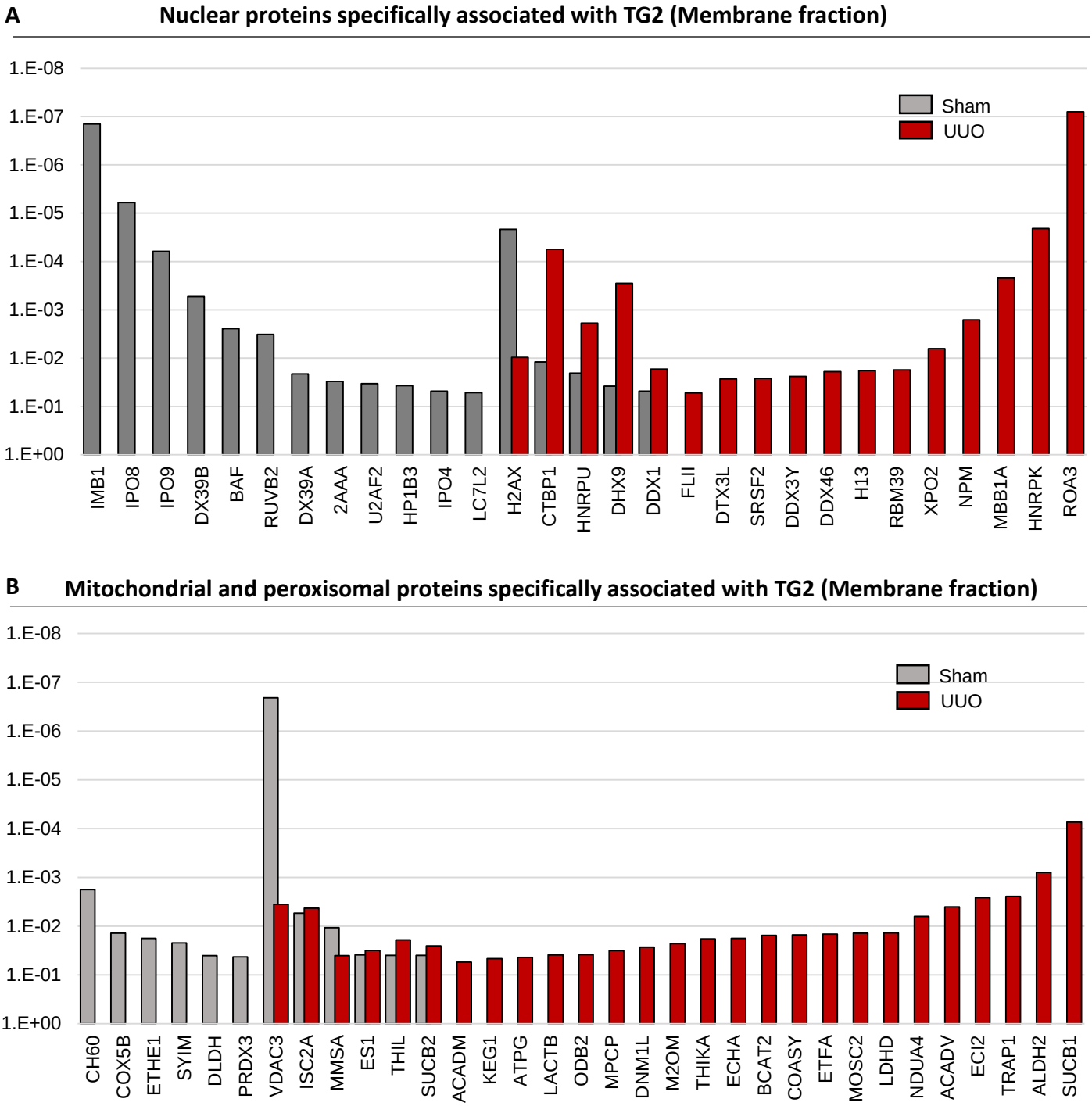

New Supplementary Figure 2

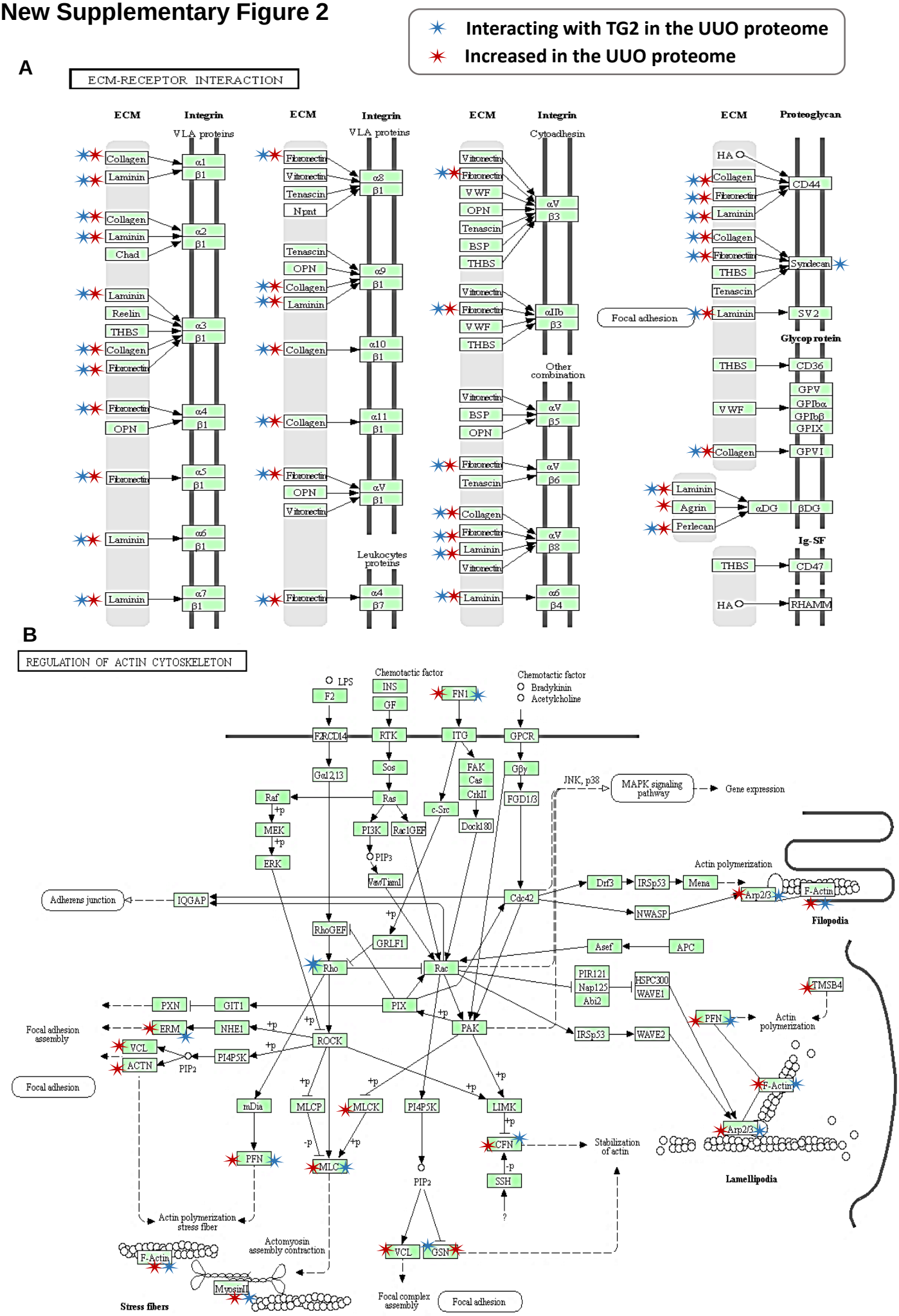

Supplementary Figure 3

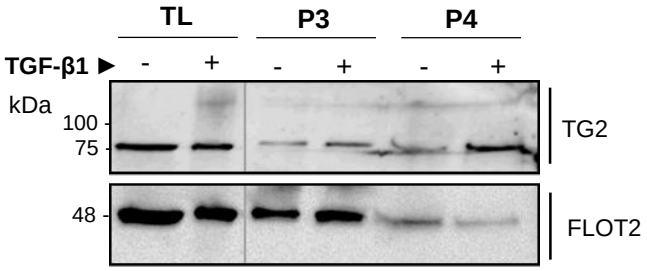

New Supplementary Figure 4

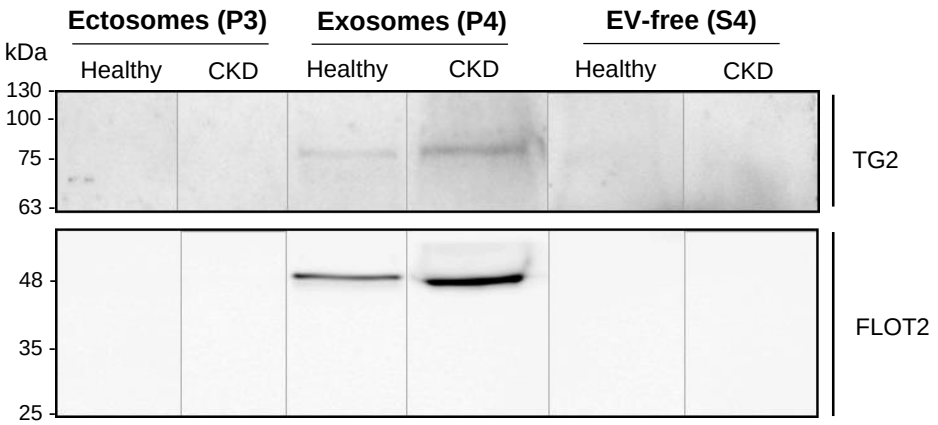

Supplementary Table 1

Ribosomal proteins specifically associated with TG2

A

UUO kidney (membrane fraction)				
Sample ID	**Name**	**N**	**P value**	**U/S**
RL3_MOUSE	60S ribosomal protein L3	5	1.26E-09	U/S
RS7_MOUSE	40S ribosomal protein S7	5	5.39E-06	U/S
RS13_MOUSE	40S ribosomal protein S13	5	3.03E-05	U/S
RS3_MOUSE	40S ribosomal protein S3	5	5.17E-05	U/S
RL6_MOUSE	60S ribosomal protein L6	5	1.36E-04	U/S
RL18A_MOUSE	60S ribosomal protein L18a	5	4.63E-04	U
RS6_MOUSE	40S ribosomal protein S6	5	2.49E-03	U/S
RLA2_MOUSE	60S acidic ribosomal protein P2	5	2.80E-03	U
RLA0_MOUSE	60S acidic ribosomal protein P0	5	2.92E-03	U/S
RL35A_MOUSE	60S ribosomal protein L35a	5	3.22E-03	U
RL18A_MOUSE	60S ribosomal protein L18a	5	3.40E-03	U
RS14_MOUSE	40S ribosomal protein S14	5	6.38E-03	U/S
RL23_MOUSE	60S ribosomal protein L23	5	7.99E-03	U
RL11_MOUSE	60S ribosomal protein L11	5	8.87E-03	U
RL10A_MOUSE	60S ribosomal protein L10a	5	9.04E-03	U
RL9_MOUSE	60S ribosomal protein L9	5	1.04E-02	U
RL17_MOUSE	60S ribosomal protein L17	5	1.05E-02	U
RS24_MOUSE	40S ribosomal protein S24	5	1.13E-02	U
RL8_MOUSE	60S ribosomal protein L8	5	1.91E-02	U
RL4_MOUSE	60S ribosomal protein L4	5	2.54E-02	U
RL23A_MOUSE	60S ribosomal protein L23a	5	2.70E-02	U
RS15_MOUSE	40S ribosomal protein S15	5	2.71E-02	U
RL40_MOUSE	Ubiquitin-60S ribosomal protein L40	5	3.64E-02	U
RL13A_MOUSE	60S ribosomal protein L13a	5	4.35E-02	U

B

Sham operated kidney (membrane fraction)				
Sample ID	**Name**	**N**	**P value**	**U/S**
RS17_MOUSE	40S ribosomal protein S17	5	4.03E-03	S
RL6_MOUSE	60S ribosomal protein L6	5	6.05E-03	U/S
RL3_MOUSE	60S ribosomal protein L3	5	6.23E-03	U/S
RS3_MOUSE	40S ribosomal protein S3	5	9.02E-03	U/S
RS13_MOUSE	40S ribosomal protein S13	5	1.21E-02	U/S
RLA0_MOUSE	60S acidic ribosomal protein P0	5	1.30E-02	U/S
RS14_MOUSE	40S ribosomal protein S14	5	2.48E-02	U/S
RS6_MOUSE	40S ribosomal protein S6	5	2.73E-02	U/S
RS7_MOUSE	40S ribosomal protein S7	5	3.52E-02	U/S

Immunoglobulin proteins specifically associated with TG2

C

UUO kidney (membrane fraction)				
Sample ID	**Name**	**N**	**P value**	**U/S**
LAC2_MOUSE	Ig lambda-1 chain C region	5	2.66E-03	U
HVM32_MOUSE	Ig heavy chain V-III region J606	5	2.30E-02	U

New Supplementary Table 2:

UUO kidney proteome – UUO / Sham > 1 (Confidence > 80%)

Protein ID	UUO/Sham	Confidence
UROM_MOUSE	16.34	0.85
COCA1_MOUSE	15.92	0.82
FBN1_MOUSE	10.84	0.89
FBLN2_MOUSE	9.65	0.81
K1C19_MOUSE	9.57	0.86
TAGL_MOUSE	9.27	0.89
PGS1_MOUSE	8.73	0.86
CNN1_MOUSE	8.59	0.80
VIME_MOUSE	8.56	0.90
HA2U_MOUSE	8.32	0.80
ANXA1_MOUSE	8.17	0.84
MT2_MOUSE	8.11	0.84
POSTN_MOUSE	8.04	0.80
A1AT2_MOUSE	7.86	0.82
FINC_MOUSE	7.85	0.84
COR1A_MOUSE	7.77	0.80
CO3A1_MOUSE	7.72	0.92
PLSL_MOUSE	7.63	0.85
CO1A1_MOUSE	7.61	0.96
KCRB_MOUSE	7.56	0.83
FBN2_MOUSE	7.26	0.94
MIME_MOUSE	6.67	0.83
CKAP4_MOUSE	6.57	0.85
LUM_MOUSE	6.55	0.87
FBLN3_MOUSE	6.33	0.80
SERPH_MOUSE	6.19	0.94
CNN2_MOUSE	6.15	0.80
LEG1_MOUSE	6.15	0.87
DESM_MOUSE	5.98	0.94
FBLN5_MOUSE	5.81	0.84
RET1_MOUSE	5.56	0.83
PDLI7_MOUSE	5.40	0.81
CLUS_MOUSE	5.35	0.81
K2C5_MOUSE	5.24	0.83
FLNA_MOUSE	5.07	0.93
MYOF_MOUSE	4.99	0.86
K2C8_MOUSE	4.93	0.89
CO6A1_MOUSE	4.78	0.88
CO6A2_MOUSE	4.76	0.94
ANXA3_MOUSE	4.73	0.83
FIBA_MOUSE	4.64	0.90
COEA1_MOUSE	4.62	0.81
HEMO_MOUSE	4.60	0.86
CSRP1_MOUSE	4.52	0.89
CO4A2_MOUSE	4.50	0.80
FIBG_MOUSE	4.45	0.85
EMIL1_MOUSE	4.42	0.82
TBA1A_MOUSE	4.41	0.96
TYB4_MOUSE	4.35	0.88
TPM1_MOUSE	4.28	0.84
K2C7_MOUSE	4.27	0.88
PEDF_MOUSE	4.24	0.81
ACTN1_MOUSE	4.22	0.96
TPM4_MOUSE	4.19	0.91
IGKC_MOUSE	4.15	0.87
FIBB_MOUSE	4.00	0.86
MYADM_MOUSE	4.00	0.87
SH3L3_MOUSE	3.85	0.90
TRFE_MOUSE	3.78	0.91
ANXA2_MOUSE	3.76	0.90
G6PE_MOUSE	3.71	0.90
CALU_MOUSE	3.69	0.84
SPB6_MOUSE	3.56	0.89
CRIP1_MOUSE	3.55	0.90
EFHD2_MOUSE	3.52	0.87
ESYT1_MOUSE	3.52	0.82
LMNA_MOUSE	3.49	0.94
CO4B_MOUSE	3.44	0.86
ARC1B_MOUSE	3.38	0.87
TBB5_MOUSE	3.33	0.88
APOE_MOUSE	3.31	0.87
MYH11_MOUSE	3.28	0.87
MYH10_MOUSE	3.27	0.85
FETUA_MOUSE	3.27	0.90
ESYT2_MOUSE	3.23	0.86
GCAB_MOUSE	3.21	0.91
ACTA_MOUSE	3.17	0.94
VTDB_MOUSE	3.13	0.93
EST1C_MOUSE	3.11	0.95
KNG1_MOUSE	3.09	0.91
MYL9_MOUSE	3.08	0.98
S10AB_MOUSE	3.08	0.88
A1AT1_MOUSE	3.07	0.86
IGG2B_MOUSE	3.07	0.81
SH3L1_MOUSE	3.06	0.86
K2C79_MOUSE	3.05	0.91
TAGL2_MOUSE	3.04	0.88
K1C18_MOUSE	2.99	0.94
ALBU_MOUSE	2.98	0.92
PTRF_MOUSE	2.96	0.84
VAT1_MOUSE	2.96	0.90
SEPT7_MOUSE	2.95	0.82
PSME2_MOUSE	2.91	0.88
B2MG_MOUSE	2.88	0.82
CERU_MOUSE	2.86	0.80
EPT2_MOUSE	2.83	0.82
COF1_MOUSE	2.74	0.87
A1AT4_MOUSE	2.72	0.83
ANXA6_MOUSE	2.71	0.89
ADPRH_MOUSE	2.71	0.86
DPYL2_MOUSE	2.68	0.88
CO4A1_MOUSE	2.67	0.88
MAP4_MOUSE	2.66	0.82
CATD_MOUSE	2.65	0.82
GBG2_MOUSE	2.65	0.81
ROA1_MOUSE	2.63	0.88
ISG15_MOUSE	2.62	0.84
FETUB_MOUSE	2.61	0.89
MYH9_MOUSE	2.61	0.99
CO3_MOUSE	2.59	0.87
MYLK_MOUSE	2.59	0.80
S10AA_MOUSE	2.59	0.86
VMA5A_MOUSE	2.58	0.86
COIA1_MOUSE	2.57	0.96
MYL6_MOUSE	2.53	0.92
CATZ_MOUSE	2.53	0.86
SF3B3_MOUSE	2.51	0.83
APOA4_MOUSE	2.50	0.82
CAP1_MOUSE	2.50	0.92
APOH_MOUSE	2.50	0.80
APOA1_MOUSE	2.46	0.92
SET_MOUSE	2.46	0.83
SFPQ_MOUSE	2.44	0.81
RBM3_MOUSE	2.36	0.84
T22D1_MOUSE	2.35	0.90
TIF1B_MOUSE	2.33	0.83
GELS_MOUSE	2.33	0.84
VINC_MOUSE	2.33	0.94
ML12B_MOUSE	2.33	0.83
LMNB1_MOUSE	2.30	0.86
ANXA5_MOUSE	2.29	0.84
PSME1_MOUSE	2.28	0.84
ANT3_MOUSE	2.27	0.86
LAMA5_MOUSE	2.26	0.83
COR1C_MOUSE	2.23	0.83
CAPZB_MOUSE	2.23	0.89
FUS_MOUSE	2.22	0.80
AGRIN_MOUSE	2.16	0.92
AN32B_MOUSE	2.15	0.81
KHDR1_MOUSE	2.14	0.84
PROF1_MOUSE	2.10	0.89
NID1_MOUSE	2.10	0.92
H2AV_MOUSE	2.07	0.86
COR1B_MOUSE	2.06	0.86
A2M_MOUSE	2.05	0.85
INO1_MOUSE	2.03	0.81
LIMA1_MOUSE	2.02	0.87
GNAI2_MOUSE	2.02	0.83
ARPC3_MOUSE	2.01	0.87
WDR1_MOUSE	2.01	0.83
UBC9_MOUSE	1.97	0.91
HP1B3_MOUSE	1.94	0.83
ACTBL_MOUSE	1.91	0.84
ROA3_MOUSE	1.90	0.90
NONO_MOUSE	1.90	0.91
ABCB7_MOUSE	1.89	0.89
ARP3_MOUSE	1.89	0.95
ARPC2_MOUSE	1.87	0.83
NH2L1_MOUSE	1.86	0.81
LAMC1_MOUSE	1.85	0.93
LAMB1_MOUSE	1.85	0.85
HNRPF_MOUSE	1.82	0.83
FABP4_MOUSE	1.82	0.85
LASP1_MOUSE	1.81	0.81
PGBM_MOUSE	1.80	0.81
TADBP_MOUSE	1.80	0.81
NUCL_MOUSE	1.79	0.83
DX39B_MOUSE	1.78	0.81
ANXA4_MOUSE	1.78	0.85
TLN1_MOUSE	1.78	0.82
FUBP2_MOUSE	1.78	0.80
ARP2_MOUSE	1.76	0.88
RUXF_MOUSE	1.75	0.87
HNRPM_MOUSE	1.74	0.86
CSRP2_MOUSE	1.72	0.82
TGM2_MOUSE	1.71	0.90
LAP2B_MOUSE	1.71	0.80
SRSF2_MOUSE	1.70	0.86
PDIA6_MOUSE	1.68	0.90
1433G_MOUSE	1.65	0.81
SMAP_MOUSE	1.64	0.88
LSM3_MOUSE	1.62	0.91
RSU1_MOUSE	1.59	0.84
SC11A_MOUSE	1.59	0.80
ABRAL_MOUSE	1.56	0.80
ACTB_MOUSE	1.56	0.93
HNRPU_MOUSE	1.53	0.85
MOES_MOUSE	1.52	0.81
GDIR1_MOUSE	1.51	0.84
HNRH1_MOUSE	1.48	0.87
SMD2_MOUSE	1.47	0.81
KAPCA_MOUSE	1.44	0.89
PDIA4_MOUSE	1.40	0.80
HNRPK_MOUSE	1.40	0.82
LAMP1_MOUSE	1.38	0.81

New Supplementary Table 3

UUO kidney proteome – UUO / Sham < 1 (Confidence > 80%)

Protein ID	Sham/UUO	Confidence
G6PC_MOUSE	72.24	0.86
AADAT_MOUSE	48.00	0.84
PDZ1I_MOUSE	45.76	0.84
HAOX2_MOUSE	44.28	0.85
CALB1_MOUSE	32.07	0.91
ASSY_MOUSE	21.28	0.88
ACSM1_MOUSE	20.87	0.83
F16P1_MOUSE	20.84	0.81
ACSM2_MOUSE	20.17	0.86
ECHP_MOUSE	19.92	0.84
KAD4_MOUSE	19.83	0.89
AT1B1_MOUSE	19.55	0.87
CAD16_MOUSE	19.54	0.92
PYC_MOUSE	18.04	0.87
GSTA2_MOUSE	17.14	0.85
AL8A1_MOUSE	17.11	0.88
ATNG_MOUSE	16.80	0.90
UD3A2_MOUSE	16.72	0.83
S100G_MOUSE	16.59	0.90
ACS2L_MOUSE	16.56	0.89
KEG1_MOUSE	16.36	0.88
SC5A2_MOUSE	16.23	0.80
ECHD2_MOUSE	16.09	0.87
CGL_MOUSE	16.04	0.86
3HAO_MOUSE	15.56	0.85
S27A2_MOUSE	14.88	0.81
MEP1B_MOUSE	14.72	0.82
ACADM_MOUSE	14.48	0.86
TMM27_MOUSE	14.41	0.85
ISC2A_MOUSE	14.27	0.90
BDH_MOUSE	14.24	0.89
ALDOB_MOUSE	14.21	0.93
HOT_MOUSE	14.07	0.84
GATM_MOUSE	13.91	0.87
GABT_MOUSE	13.84	0.93
KBL_MOUSE	13.82	0.85
MMSA_MOUSE	13.79	0.88
PXMP2_MOUSE	13.77	0.81
ST1D1_MOUSE	13.74	0.85
GGT1_MOUSE	13.58	0.89
MAAI_MOUSE	13.49	0.82
PGAM2_MOUSE	13.44	0.88
GLYAT_MOUSE	13.43	0.88
S4A4_MOUSE	13.29	0.83
FAAA_MOUSE	13.16	0.92
AT1A1_MOUSE	13.14	0.93
DHSO_MOUSE	13.11	0.82
MPC1_MOUSE	12.91	0.93
UK114_MOUSE	12.69	0.94
ACE_MOUSE	12.66	0.91
DECR2_MOUSE	12.62	0.90
CATA_MOUSE	12.62	0.94
ACY3_MOUSE	12.43	0.80
S22A2_MOUSE	12.29	0.81
GSTK1_MOUSE	12.27	0.82
PCCB_MOUSE	12.22	0.96
AL4A1_MOUSE	12.17	0.93
CES1D_MOUSE	11.96	0.83
GLPK_MOUSE	11.89	0.86
QORL2_MOUSE	11.85	0.82
AAAD_MOUSE	11.84	0.85
VILI_MOUSE	11.78	0.91
DHAK_MOUSE	11.77	0.80
COX1_MOUSE	11.70	0.90
SODM_MOUSE	11.66	0.93
S2542_MOUSE	11.63	0.86
MPC2_MOUSE	11.60	0.82
ATP5L_MOUSE	11.54	0.80
OXDA_MOUSE	11.38	0.81
NUD19_MOUSE	11.28	0.90
HINT2_MOUSE	11.27	0.98
BPHL_MOUSE	11.09	0.87
MCCB_MOUSE	10.95	0.90
PBLD1_MOUSE	10.91	0.87
DIC_MOUSE	10.83	0.83
ACD10_MOUSE	10.77	0.86
NHRF3_MOUSE	10.71	0.86
GSTA3_MOUSE	10.63	0.81
CK054_MOUSE	10.61	0.82
AK1A1_MOUSE	10.56	0.91
3HIDH_MOUSE	10.55	0.94
SUCB2_MOUSE	10.42	0.94
LACB2_MOUSE	10.39	0.82
FAHD1_MOUSE	10.39	0.84
FMO1_MOUSE	10.33	0.82
IVD_MOUSE	10.14	0.88
THIL_MOUSE	10.10	0.95
PROD_MOUSE	10.05	0.81
SARDH_MOUSE	10.05	0.85
INMT_MOUSE	10.03	0.83
AL1L1_MOUSE	9.95	0.91
KHK_MOUSE	9.90	0.83
ARK72_MOUSE	9.87	0.87
S22AI_MOUSE	9.86	0.90
HCDH_MOUSE	9.82	0.90
NDUB6_MOUSE	9.77	0.81
CISD1_MOUSE	9.75	0.95
NDRG1_MOUSE	9.52	0.99
S13A3_MOUSE	9.52	0.88
CYC_MOUSE	9.49	0.92
SSDH_MOUSE	9.47	0.88
SCOT1_MOUSE	9.34	0.92
HMGCL_MOUSE	9.26	0.92
ACPM_MOUSE	9.19	0.92
ATPK_MOUSE	9.17	0.80
MSRA_MOUSE	9.12	0.83
CBR1_MOUSE	9.11	0.92
LDHD_MOUSE	9.10	0.88
COX5A_MOUSE	9.08	0.94
ETFA_MOUSE	9.07	0.93
NDUB5_MOUSE	9.01	0.85
PLSI_MOUSE	9.01	0.86
GPDA_MOUSE	8.85	0.91
NIPS1_MOUSE	8.81	0.91
NU4M_MOUSE	8.79	0.89
FAHD2_MOUSE	8.76	0.80
CLYBL_MOUSE	8.75	0.80
FBX50_MOUSE	8.73	0.80
NDUS6_MOUSE	8.72	0.81
THNS2_MOUSE	8.70	0.83
NDUB8_MOUSE	8.67	0.86
NU5M_MOUSE	8.67	0.88
PECR_MOUSE	8.65	0.87
SDHA_MOUSE	8.64	0.98
NDUBA_MOUSE	8.63	0.86
SUCA_MOUSE	8.55	0.94
NDUV2_MOUSE	8.50	0.84
IPYR2_MOUSE	8.50	0.83
NDUV1_MOUSE	8.43	0.90
NDUA9_MOUSE	8.38	0.89
ABCD3_MOUSE	8.36	0.88
ATPD_MOUSE	8.32	0.98
QCR6_MOUSE	8.31	0.93
NDUA1_MOUSE	8.25	0.86
COX5B_MOUSE	8.24	0.91
IDHP_MOUSE	8.21	0.93
SBP1_MOUSE	8.19	0.92
NDUS7_MOUSE	8.16	0.94
BDH2_MOUSE	8.13	0.82
ETFB_MOUSE	8.13	0.91
NHRF1_MOUSE	8.07	0.94
NEP_MOUSE	8.05	0.90
NDUAD_MOUSE	8.00	0.89
CSAD_MOUSE	8.00	0.90
COX2_MOUSE	7.99	0.87
SDHB_MOUSE	7.99	0.89
TPMT_MOUSE	7.98	0.93
CY1_MOUSE	7.96	0.94
TOM5_MOUSE	7.94	1.00
COQ9_MOUSE	7.91	0.90
IDHG1_MOUSE	7.91	0.91
THIM_MOUSE	7.90	0.91
UCRI_MOUSE	7.89	0.91
NDUA3_MOUSE	7.86	0.89
AUHM_MOUSE	7.85	0.85
COASY_MOUSE	7.83	0.85
NLTP_MOUSE	7.82	0.88
NDUB7_MOUSE	7.79	0.84
TAU_MOUSE	7.76	0.83
THTR_MOUSE	7.75	0.89
PPA6_MOUSE	7.74	0.85
QOR_MOUSE	7.71	0.84
ACSL1_MOUSE	7.69	0.90
CRYL1_MOUSE	7.62	0.90
LRP2_MOUSE	7.60	0.84
CX7A1_MOUSE	7.60	0.93
HGD_MOUSE	7.58	0.84
CH60_MOUSE	7.56	0.96
C560_MOUSE	7.55	0.83
NDUS1_MOUSE	7.55	0.94
CP013_MOUSE	7.48	0.87
COX41_MOUSE	7.46	0.94
ACD11_MOUSE	7.41	0.80
CX7A2_MOUSE	7.37	0.92
NAKD2_MOUSE	7.33	0.95
VATG1_MOUSE	7.31	0.83
NDUA4_MOUSE	7.30	0.89
AIFM1_MOUSE	7.30	0.92
CDD_MOUSE	7.28	0.81
MUTA_MOUSE	7.27	0.81
MCCA_MOUSE	7.25	0.82
NDUB4_MOUSE	7.21	0.83
ECHM_MOUSE	7.21	0.90
ATP5H_MOUSE	7.21	0.93
OCTC_MOUSE	7.20	0.80
CMC2_MOUSE	7.20	0.80
NDUS4_MOUSE	7.19	0.83
CBR4_MOUSE	7.19	0.85
DLDH_MOUSE	7.18	0.94
AL7A1_MOUSE	7.16	0.82
MEP1A_MOUSE	7.15	0.88
QCR2_MOUSE	7.14	0.94
C1TC_MOUSE	7.12	0.87
QCR8_MOUSE	7.12	0.91
MGST3_MOUSE	7.12	0.84
ADT2_MOUSE	7.06	0.81
ATP8_MOUSE	6.97	0.90
ATPG_MOUSE	6.96	0.90
NDUAA_MOUSE	6.92	0.93
S12A1_MOUSE	6.91	0.96
AQP1_MOUSE	6.91	0.80
ODO2_MOUSE	6.89	0.89
TBA4A_MOUSE	6.89	0.88
ATPO_MOUSE	6.84	0.96
PCCA_MOUSE	6.83	0.84
BPNT1_MOUSE	6.81	0.87
PTER_MOUSE	6.73	0.91
FGGY_MOUSE	6.73	0.85
ECI2_MOUSE	6.73	0.85
NDUS2_MOUSE	6.72	0.91
ES1_MOUSE	6.71	0.92
ACON_MOUSE	6.66	0.90
NDUS3_MOUSE	6.64	0.96
MDHM_MOUSE	6.63	0.96
ATP5I_MOUSE	6.62	0.90
USMG5_MOUSE	6.60	0.97
FUMH_MOUSE	6.56	0.89
ATPB_MOUSE	6.55	0.94
FABPH_MOUSE	6.53	0.88
AQP3_MOUSE	6.51	0.90
CX6B1_MOUSE	6.48	0.92
NDUA5_MOUSE	6.48	0.90
VWA8_MOUSE	6.46	0.82
ATPA_MOUSE	6.46	0.96
DHRS4_MOUSE	6.42	0.91
SUSD2_MOUSE	6.38	0.92
QCR1_MOUSE	6.37	0.94
NDUA7_MOUSE	6.36	0.91
SFXN1_MOUSE	6.35	0.83
QCR7_MOUSE	6.34	0.89
COX6C_MOUSE	6.33	0.91

Protein ID	Sham/UUO	Confidence
ODB2_MOUSE	6.31	0.81
ARLY_MOUSE	6.31	0.91
PRDX5_MOUSE	6.30	0.91
PGES2_MOUSE	6.29	0.89
ATP5J_MOUSE	6.29	0.97
KAT3_MOUSE	6.29	0.81
ACOX2_MOUSE	6.24	0.84
AT5F1_MOUSE	6.17	0.92
NU3M_MOUSE	6.15	0.95
CH10_MOUSE	6.15	0.90
NDUB9_MOUSE	6.10	0.83
AATM_MOUSE	6.10	0.97
DHB8_MOUSE	6.07	0.87
NDUA8_MOUSE	6.07	0.91
CHDH_MOUSE	6.06	0.88
ODPB_MOUSE	6.05	0.96
VATA_MOUSE	6.04	0.92
MRP2_MOUSE	6.03	0.82
ETHE1_MOUSE	5.99	0.92
VATH_MOUSE	5.94	0.90
NDUC2_MOUSE	5.93	0.88
DCXR_MOUSE	5.92	0.88
GSTT2_MOUSE	5.84	0.87
ALDH2_MOUSE	5.82	0.95
TRAP1_MOUSE	5.82	0.88
AL9A1_MOUSE	5.76	0.94
ETFD_MOUSE	5.74	0.89
CPT2_MOUSE	5.70	0.88
ANK3_MOUSE	5.70	0.85
ACOT4_MOUSE	5.68	0.81
MARC2_MOUSE	5.65	0.89
ACOT1_MOUSE	5.63	0.85
DOPD_MOUSE	5.63	0.91
TIM13_MOUSE	5.58	0.96
ODPA_MOUSE	5.58	0.92
MPCP_MOUSE	5.57	0.90
ABHEB_MOUSE	5.57	0.93
GRP75_MOUSE	5.56	0.82
HIBCH_MOUSE	5.55	0.89
NDUBB_MOUSE	5.53	0.90
MIC19_MOUSE	5.53	0.90
VATB2_MOUSE	5.52	0.85
GSH1_MOUSE	5.49	0.86
NCEH1_MOUSE	5.47	0.92
ECH1_MOUSE	5.46	0.97
VATF_MOUSE	5.45	0.90
VATG3_MOUSE	5.43	0.94
CN159_MOUSE	5.41	0.83
DECR_MOUSE	5.39	0.89
CMBL_MOUSE	5.38	0.85
ACADS_MOUSE	5.36	0.89
SUCB1_MOUSE	5.33	0.97
VATE1_MOUSE	5.32	0.91
LPPRC_MOUSE	5.26	0.88
ODP2_MOUSE	5.25	0.98
PRDX3_MOUSE	5.23	0.90
KAD2_MOUSE	5.21	0.86
SQRD_MOUSE	5.20	0.92
GSHB_MOUSE	5.17	0.82
LYPA1_MOUSE	5.13	0.90
ACADV_MOUSE	5.12	0.89
KAD3_MOUSE	5.10	0.89
DHPR_MOUSE	5.07	0.88
NIT1_MOUSE	5.03	0.90
ODO1_MOUSE	5.00	0.91
E41L3_MOUSE	4.96	0.86
SAP3_MOUSE	4.96	0.85
MDHC_MOUSE	4.94	0.95
SPS2_MOUSE	4.93	0.90
THIOM_MOUSE	4.90	0.90
RM12_MOUSE	4.89	0.91
NIT2_MOUSE	4.88	0.90
IDH3A_MOUSE	4.86	0.91
NDUA6_MOUSE	4.86	0.84
VDAC1_MOUSE	4.85	0.96
HYES_MOUSE	4.85	0.81
ACOC_MOUSE	4.84	0.94

Protein ID	Sham/UUO	Confidence
PH4H_MOUSE	4.83	0.84
ECI1_MOUSE	4.80	0.91
HCD2_MOUSE	4.76	0.91
IDHC_MOUSE	4.75	0.90
ISCA2_MOUSE	4.73	0.82
MIC27_MOUSE	4.70	0.81
SAM50_MOUSE	4.69	0.89
LONM_MOUSE	4.66	0.90
MIC60_MOUSE	4.65	0.92
ATIF1_MOUSE	4.61	0.83
LYZ2_MOUSE	4.60	0.93
OAT_MOUSE	4.59	0.86
DDAH1_MOUSE	4.57	0.83
EFTU_MOUSE	4.54	0.95
CMC1_MOUSE	4.51	0.84
ECHA_MOUSE	4.46	0.97
RT35_MOUSE	4.43	0.81
THTM_MOUSE	4.41	0.83
XPP1_MOUSE	4.40	0.87
VATD_MOUSE	4.40	0.89
BCAT2_MOUSE	4.38	0.89
DHE3_MOUSE	4.37	0.92
4F2_MOUSE	4.34	0.91
ATAD3_MOUSE	4.30	0.80
TRXR2_MOUSE	4.29	0.83
ACADL_MOUSE	4.28	0.87
CPT1A_MOUSE	4.27	0.84
KCRU_MOUSE	4.24	0.88
AMPE_MOUSE	4.21	0.87
GLRX5_MOUSE	4.20	0.93
MAOX_MOUSE	4.20	0.83
M2OM_MOUSE	4.19	0.83
CLIC5_MOUSE	4.18	0.85
ACDSB_MOUSE	4.10	0.93
BASI_MOUSE	4.09	0.87
SCRN2_MOUSE	4.05	0.82
TMM65_MOUSE	4.03	0.88
TIM10_MOUSE	4.01	0.86
MTCH2_MOUSE	4.01	0.89
PROSC_MOUSE	4.01	0.90
LDHB_MOUSE	3.99	0.86
MOT1_MOUSE	3.98	0.91
MAVS_MOUSE	3.95	0.84
T126A_MOUSE	3.93	0.85
GLNA_MOUSE	3.91	0.83
CYB5_MOUSE	3.87	0.86
AT11A_MOUSE	3.85	0.81
CISY_MOUSE	3.83	0.88
AMPN_MOUSE	3.83	0.95
ADT1_MOUSE	3.82	0.83
EM55_MOUSE	3.82	0.91
PTGR2_MOUSE	3.79	0.89
NPL_MOUSE	3.76	0.88
PHB2_MOUSE	3.73	0.94
MIF_MOUSE	3.71	0.92
EBP_MOUSE	3.70	0.91
AATC_MOUSE	3.68	0.88
DHI2_MOUSE	3.67	0.83
TSPO_MOUSE	3.66	0.98
NCPR_MOUSE	3.64	0.81
CYB5B_MOUSE	3.62	0.93
THIC_MOUSE	3.61	0.85
GSTA4_MOUSE	3.61	0.86
RM04_MOUSE	3.59	0.91
AMPL_MOUSE	3.57	0.93
VATC1_MOUSE	3.55	0.83
GGCT_MOUSE	3.55	0.99
C1QBP_MOUSE	3.52	0.83
ACBP_MOUSE	3.51	0.93
EFTS_MOUSE	3.50	0.85
TXTP_MOUSE	3.47	0.87
SPRE_MOUSE	3.47	0.96
GPX1_MOUSE	3.45	0.92
F213A_MOUSE	3.42	0.89
DHB4_MOUSE	3.39	0.95
ECHB_MOUSE	3.37	0.87
SODC_MOUSE	3.33	0.94

Protein ID	Sham/UUO	Confidence
NAPSA_MOUSE	3.32	0.84
ESTD_MOUSE	3.28	0.86
APMAP_MOUSE	3.28	0.84
GSTM5_MOUSE	3.27	0.87
PGK1_MOUSE	3.27	0.97
ISCU_MOUSE	3.25	0.81
VA0D1_MOUSE	3.24	0.87
GVIN1_MOUSE	3.22	0.83
PRPS2_MOUSE	3.20	0.85
PGM1_MOUSE	3.13	0.90
PHB_MOUSE	3.13	0.92
EZRI_MOUSE	3.13	0.96
EHD1_MOUSE	3.05	0.83
HINT1_MOUSE	3.04	0.88
SAHH_MOUSE	2.99	0.91
GNPI1_MOUSE	2.96	0.89
CAH2_MOUSE	2.95	0.95
THIKA_MOUSE	2.95	0.91
HDHD2_MOUSE	2.90	0.82
TTC38_MOUSE	2.87	0.87
41_MOUSE	2.84	0.85
VDAC2_MOUSE	2.84	0.94
HEM2_MOUSE	2.82	0.91
RADI_MOUSE	2.79	0.83
CCS_MOUSE	2.75	0.99
AKCL2_MOUSE	2.73	0.93
GPD1L_MOUSE	2.72	0.87
TPIS_MOUSE	2.71	0.95
UGPA_MOUSE	2.66	0.87
HXK1_MOUSE	2.66	0.91
FIS1_MOUSE	2.65	0.89
GLGB_MOUSE	2.59	0.98
GTR1_MOUSE	2.58	0.80
NAMPT_MOUSE	2.57	0.82
FUCM_MOUSE	2.52	0.88
ENOA_MOUSE	2.51	0.98
SYPL1_MOUSE	2.50	0.91
S10A1_MOUSE	2.44	0.85
PDXK_MOUSE	2.42	0.85
PARK7_MOUSE	2.42	0.93
PGAM1_MOUSE	2.41	0.97
GMPR1_MOUSE	2.41	0.81
GSTM1_MOUSE	2.37	0.89
EHD3_MOUSE	2.37	0.86
GSHR_MOUSE	2.33	0.80
G3P_MOUSE	2.29	0.92
TMM33_MOUSE	2.28	0.86
TIM44_MOUSE	2.25	0.83
ARL1_MOUSE	2.24	0.90
PRDX6_MOUSE	2.23	0.94
NDKB_MOUSE	2.11	0.95
ADK_MOUSE	2.03	0.87
PRDX1_MOUSE	2.03	0.91
G6PI_MOUSE	2.03	0.93
RS24_MOUSE	1.99	0.88
NDKA_MOUSE	1.98	0.88
AP1B1_MOUSE	1.97	0.82
PACN2_MOUSE	1.96	0.85
MAT2B_MOUSE	1.94	0.89
PEBP1_MOUSE	1.92	0.92
SPTN1_MOUSE	1.85	0.88
TMED4_MOUSE	1.84	0.90
SPTB2_MOUSE	1.80	0.87
UGDH_MOUSE	1.79	0.82
GSTP1_MOUSE	1.77	0.94
UAP1L_MOUSE	1.76	0.84
SNX3_MOUSE	1.72	0.84
TBB4B_MOUSE	1.71	0.90
GALK1_MOUSE	1.64	0.85
ALDOA_MOUSE	1.57	0.84
GPX3_MOUSE	1.54	0.83
HS90A_MOUSE	1.50	0.81
CLH1_MOUSE	1.47	0.88

New Supplementary Table 4

A

SIGNIFICANTLY ENRICHED PROTEIN CLASSES (PANTHER)	UUO/Sham > 1			UUO/Sham < 1		
	Fold change		p-value	Fold change		p-value
cytoskeletal protein (PC00085)	+	7.82	1.99E-28	-	0.82	1.00E+00
actin family cytoskeletal protein (PC00041)	+	11.33	2.49E-25	-	0.89	1.00E+00
extracellular matrix protein (PC00102)	+	6.76	1.92E-09	-	0.4	1.00E+00
non-motor actin binding protein (PC00165)	+	9.05	4.09E-08	-	1	1.00E+00
intermediate filament (PC00129)	+	14.19	7.22E-07	-	< 0.2	1.00E+00
extracellular matrix structural protein (PC00103)	+	14.87	2.99E-06	-	< 0.2	1.00E+00
serine protease inhibitor (PC00204)	+	8.79	1.52E-05	-	< 0.2	1.00E+00
mRNA splicing factor (PC00148)	+	9.89	2.06E-05	-	< 0.2	1.00E+00
mRNA processing factor (PC00147)	+	7.99	3.86E-05	-	< 0.2	1.00E+00
surfactant (PC00212)	+	15.36	1.01E-04	-	< 0.2	1.00E+00
structural protein (PC00211)	+	7.31	3.11E-04	-	< 0.2	1.00E+00
extracellular matrix linker protein (PC00101)	+	23.2	6.28E-04	-	< 0.2	1.00E+00
actin and actin related protein (PC00039)	+	20.8	1.06E-03	-	< 0.2	1.00E+00
protease inhibitor (PC00191)	+	4.7	2.51E-03	-	< 0.2	4.04E-01
enzyme modulator (PC00095)	+	2.22	2.48E-02	-	0.39	2.52E-02
actin binding motor protein (PC00040)	+	10.22	3.03E-02	-	< 0.2	1.00E+00
antibacterial response protein (PC00051)	+	5.95	4.21E-02	-	< 0.2	1.00E+00
transferase (PC00220)	-	< 0.2	4.95E-02	+	2.67	4.96E-11
nucleotide kinase (PC00172)	-	< 0.2	1.00E+00	+	6.23	3.35E-02
transaminase (PC00216)	-	< 0.2	1.00E+00	+	10.38	2.91E-02
G-protein coupled receptor (PC00021)	-	< 0.2	1.00E+00	-	< 0.2	1.39E-02
transporter (PC00227)	+	1.15	1.00E+00	+	1.93	4.81E-03
nucleic acid binding (PC00171)	+	1.03	1.00E+00	-	0.47	3.34E-03
peroxidase (PC00180)	-	< 0.2	1.00E+00	+	11.96	2.87E-03
transfer/carrier protein (PC00219)	+	1.41	1.00E+00	+	2.79	1.92E-03
anion channel (PC00049)	-	< 0.2	1.00E+00	+	14.23	1.08E-03
carbohydrate kinase (PC00065)	-	< 0.2	1.00E+00	+	11.25	8.17E-04
hydrolase (PC00121)	-	0.77	1.00E+00	+	1.91	2.85E-04
ligase (PC00142)	-	0.31	1.00E+00	+	3.18	1.29E-04
receptor (PC00197)	+	1.43	1.00E+00	-	0.28	4.20E-05
mitochondrial carrier protein (PC00158)	-	< 0.2	1.00E+00	+	9.61	7.16E-06
cation transporter (PC00068)	-	< 0.2	1.00E+00	+	4.87	1.06E-06
acyltransferase (PC00042)	+	1.28	1.00E+00	+	7.95	3.05E-07
epimerase/racemase (PC00096)	-	< 0.2	1.00E+00	+	12.03	5.59E-09
transcription factor (PC00218)	-	0.55	1.00E+00	-	< 0.2	2.07E-09
acetyltransferase (PC00038)	-	< 0.2	1.00E+00	+	9.41	1.90E-09
ATP synthase (PC00002)	-	< 0.2	1.00E+00	+	15.06	1.86E-09
isomerase (PC00135)	-	< 0.2	1.00E+00	+	6.99	5.53E-11
hydratase (PC00120)	-	< 0.2	1.00E+00	+	35.17	6.73E-13
lyase (PC00144)	-	< 0.2	1.00E+00	+	8.25	1.26E-13
oxidase (PC00175)	-	0.83	1.00E+00	+	9.28	2.02E-15
reductase (PC00198)	-	0.6	1.00E+00	+	10.61	1.60E-27
dehydrogenase (PC00092)	-	0.91	1.00E+00	+	16.29	3.41E-73
oxidoreductase (PC00176)	-	0.56	1.00E+00	+	10.38	1.77E-91

B

KEGG PATHWAYS SIGNIFICANTLY ENRICHED IN UUO KIDNEYS	Fold Change	p-value
mmu04510:Focal adhesion	6.36	1.29E-09
mmu04810:Regulation of actin cytoskeleton	5.48	3.82E-08
mmu04512:ECM-receptor interaction	9.27	1.89E-07
mmu04610:Complement and coagulation cascades	8.40	8.72E-06
mmu03040:Spliceosome	5.64	5.41E-05
mmu05414:Dilated cardiomyopathy	5.32	1.78E-03
mmu04530:Tight junction	4.15	2.79E-03
mmu04670:Leukocyte transendothelial migration	4.12	6.42E-03
mmu05222:Small cell lung cancer	4.94	6.72E-03
mmu05416:Viral myocarditis	4.47	1.02E-02
mmu04666:Fc gamma R-mediated phagocytosis	4.28	1.21E-02
mmu05322:Systemic lupus erythematosus	4.08	1.48E-02
mmu04270:Vascular smooth muscle contraction	3.50	2.67E-02
mmu05410:Hypertrophic cardiomyopathy (HCM)	4.17	3.03E-02